

Manufacturing of Nanochannels with Controlled Dimensions Using Protease Nanolithography

Rodica E. Ionescu, Robert S. Marks, and Levi A. Gheber*

*Department of Biotechnology Engineering, Ben-Gurion University of the Negev,
P.O. Box 653, Beer-Sheva 84105, Israel*

Received January 11, 2005

ABSTRACT

The feasibility of creating nanometer scale depressions in biological substrates using active enzymes delivered with scanning probe microscopes has been previously demonstrated by us and other groups. Here we present a comprehensive study revealing the dependence of channels dimensions on the parameters of the “writing” process and provide a simple way to precisely control their dimensions. Such nanochannels may be used in nanofluidic biochip applications.

It has been recently shown by at least three independent groups^{1–3} that active enzymes can be controllably directed to very precise locations on a surface with the aid of scanning probe microscopes (SPM) and used to create depressions in biological substrates. The techniques reported used a protease immobilized to an AFM tip to specifically cleave a protein immobilized on a surface,¹ dip-pen lithography⁴ delivered DNase to an oligonucleotide SAM on gold,³ and trypsin delivered with a nano fountain pen⁵ (NFP) to a film of BSA to create pits (wells) and trenches (channels).² The various techniques have various advantages and disadvantages, but they all prove the concept of using “smart” etchants that have specific recognition for their substrate. In addition to specificity, enzyme-based lithography offers the advantage of creating depressions (channels and/or wells) that are readily biologically functional, since the substrate into which the enzymes carve are biological molecules. Biological specific recognition, enzymatic chemical efficiency and precise positioning of minute amounts of molecules, in combination with SPM-based techniques that can pattern biological molecules, such as DNA^{6,7} and various proteins,^{8–10} may lead to impressive advances in the developing fields of nanobiochips, nanofluidics, and nano lab-on-a-chip.

We have extended our study of the trypsin–BSA model system in an attempt to understand how the dimensions of the features created may be modulated and controlled by the various parameters of deposition. We chose to work with thick films of dried BSA in order not to limit the extent of etching by consuming of substrate, but rather allow the process to naturally end. In our previous study² we have developed a model that is in excellent agreement with the

experiments and explains the details of the processes occurring during etching. The main features of the model are: (i) etching is the result of a competition between swelling of the BSA substrate and the trypsin cleavage rate; (ii) etching ends once the water evaporates and renders the trypsin inactive; (iii) the depressions are created as a result of collapse of BSA molecules following the cleavage of a sufficient number of the peptide bonds by trypsin (86 of those exist). Based on this understanding of the process, we studied the effect of varying the deposition velocity and aperture diameters on the dimensions of the channels created.

Protein Substrate. The substrate was prepared by dissolving BSA (Albumin bovine, Fraction V Sigma) in ultrapure Millipore water to a concentration of 0.5 mM and applying 35 μ L drops onto 95% ethanol flamed glass coverslips ($\varnothing = 16$ mm; Marienfeld, Germany), then allowing to dry for 7 days at room temperature.

Protease. Bovine trypsin, treated with L-(tosylamido-2-phenyl ethyl) chloromethyl ketone to inhibit chemotryptic activity (TPCK-trypsin, bovine pancreas, Pierce), in an amount of 2 mg, was diluted in 1 mL of 0.05 M sodium borate, pH = 8.5 (BupH borate buffer, Pierce) and subsequently loaded in the nanopipets (Nanonics Ltd., Jerusalem, Israel).

AFM Probes. Cantilevered AFM probes (MickroMasch, Estonia) used for surface topography imaging were made of silicon nitride, coated on the reflective side with a Cr–Au layer.

Nanopipets. Nano fountain pen writing was performed with cantilevered nanopipets (Nanonics, Jerusalem, Israel) that were held as the probe in the SPM and controlled in a fashion identical to a regular AFM probe. Writing was

* Corresponding author. E-mail: glevi@bgumail.bgu.ac.il.

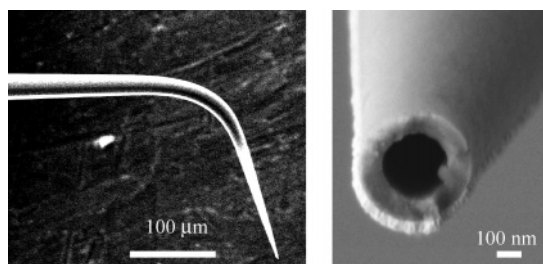


Figure 1. SEM images of a cantilevered nanopipet with 200 nm aperture.

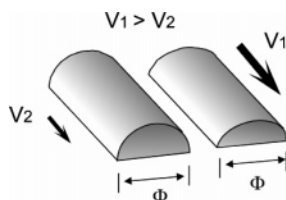


Figure 2. Two imaginary trails of trypsin solution left on the surface by a pipet with aperture diameter Φ , when writing occurs at two different velocities $V_1 > V_2$. The trails have the same width, which is of the order of magnitude of the pipet diameter; however, the trail written at V_2 (slower velocity) is taller.

performed in contact mode, after confirming the ability to scan the BSA surface without indenting it. Flow of trypsin solution was initiated by contacting the pipet with the surface and stopped by lifting it from the surface. No external pressure was applied on the liquid.

Scanning Probe Microscope. Both writing and imaging were performed with a Nanonics NSOM/AFM 100 system (Jerusalem, Israel) with a flat scanner, which allows two optical microscopes to examine the sample simultaneously, from top and bottom. This setup made it possible to follow the writing process and, subsequently, to easily position the AFM probe over the desired features for imaging.

We have used three pipet diameters, 100 nm, 200 nm and 300 nm (a SEM image of a 200 nm pipet is shown in Figure 1), and for each diameter we delivered trypsin with velocities of 1 $\mu\text{m/s}$, 1.5 $\mu\text{m/s}$, 3 $\mu\text{m/s}$, and 6 $\mu\text{m/s}$, giving a total of 12 different combinations. We used at least three pipets of each diameter and created at least 10 channels for each velocity with every single pipet. Cross-section profiles were measured in at least five positions along each channel. The control of the velocity was achieved by setting the dwelling time of the scanner for each position (pixel), and is referred to as Δt throughout.

Controlling Width and Depth Separately. We expected (naively) to observe an increase in channel depth but not much change in the channel width, with decreasing velocities, for a given pipet diameter. The main reasoning is that the width of the channel should be in some way proportional to the aperture diameter of the pipet (so that for a given pipet, the width of the channel should be approximately constant), while slow velocities will cause the delivery of more trypsin per unit length, which in turn will etch a deeper channel (see sketch in Figure 2). In addition, one would expect larger aperture pipets to create wider and deeper channels, compared with smaller aperture pipets, when the writing velocity

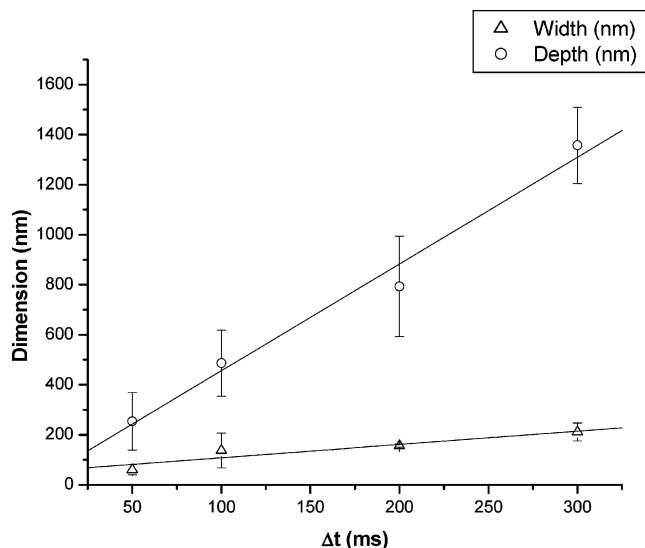


Figure 3. Dependence of the width (triangles) and of the depth (circles) of channels created with four different 200 nm pipets on the dwelling time (the time spent by the pipet in each one of 256 positions along the line). Linear fit yields width = $(0.5 \pm 0.1)\Delta t + (55 \pm 25)$ nm and depth = $(4.3 \pm 0.4)\Delta t + (29 \pm 74)$ nm.

is equal. In some instances this could be observed, to some extent. An example is shown in Figure 3, where the data represent the average of widths and depths of channels created with four different 200 nm pipets. We are plotting the width (triangles) and the depth (circles) as a function of the delay time, Δt (and not the velocity), since this produces linear plots and makes it easier to assess the behavior at $\Delta t = 0$ (rather than $V \rightarrow \infty$). It is observed that the width dependence on Δt is less than that of the depth (0.5 nm/ms compared with 4 nm/ms). Moreover, the limiting width at $\Delta t = 0$ (infinite velocity) is 55 ± 25 nm, a positive value, comparable with the nominal 200 nm pipet aperture, while the limiting depth at $\Delta t = 0$ is 29 ± 74 nm, which includes zero within the experimental error, and in fact, could even be a negative value. A negative depth means a positive height, which is consistent with our previously presented model,² i.e., a swelling stage is preceding the start of etching by trypsin. Despite the apparently well understood behavior described above, this represents only a subset of our results (~40%), while in other cases the data seem inconsistent. The discrepancies consist of inversion of the slopes in some instances (the dependence on velocity is stronger for width than for depth) or inconsistencies among different apertures (narrower channels for wider apertures and vice versa). We attribute the general spread of data to inhomogeneous (and anisotropic) density of the BSA film. Thus, in different regions of the film etching proceeds at different rates in the horizontal (x,y) and vertical (z) directions, giving rise to discrepancies when the data is analyzed in terms of width and depth separately. In the following we are showing that all of the data for all pipets, all writing velocities, and all channels created can be presented in a consistent way, in terms of more appropriate variables.

Controlling the Cross-Section Area. The way to interpret the data is by assuming that the volume of trypsin solution

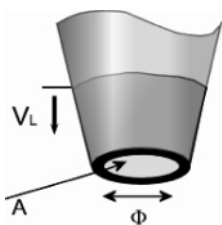


Figure 4. Definition of the parameters used in the model: Φ is the pipet aperture diameter, A is the area of the pipet aperture ($\pi\Phi^2/4$), and V_L is the linear velocity of liquid flow out of the pipet.

delivered to the surface is proportional to the volume of the depression created in the BSA film. If one assumes the solution flows out of the pipet with a constant linear velocity, V_L (see Figure 4), then the volume of solution delivered to the surface is proportional to the aperture area multiplied by the duration of flow ($A\Delta t$). The delivered volume thus will be calculated as $V_L A\Delta t$. This solution will etch a volume proportional to its own, according to the assumption. Therefore, since the pipet advances in steps (256 steps per line) and dwells in each position a known time duration (Δt), the etched volume can be calculated as the area of the channel cross-section (CS), measured from cross sections of the topography image, multiplied by the size of a pixel (Ps), in our case, $77 \mu\text{m}/256 \text{ pixels} \approx 300 \text{ nm}$. Therefore, we should have

$$\text{CS} \times \text{Ps} = K V_L A \Delta t$$

where CS is cross-sectional area of the channel, Ps is pixel size (scan range divided by number of pixels per line), V_L is a (constant) linear velocity of flow of the solution from the pipet, A is the area of the pipet aperture, Δt is the time the pipet spends in one position (dwell time), and K is a (dimensionless) constant describing the ratio of the etched volume to delivered volume of trypsin solution. Since Ps, K , and V_L are (presumably) constant, one expects a linear dependence of the channel cross-sectional area on the product $A\Delta t$.

Indeed, as shown in Figure 5, one observes a very clear trend for each pipet diameter, indicating that our model explains well the data. It is important to note that all of the data, with no exceptions, are presented in Figure 5, including the subset presented in Figure 3. As previously mentioned, the reason that the data for depth and width separately are not consistent, except in certain cases, is probably that, due to inhomogeneous density of the BSA film, the etching rate of trypsin in the lateral and vertical directions varies from place to place. Therefore, even for the very same pipet, when creating various channels that are separated by some distance, it may so happen that the width and depth of one channel differ from those of the neighboring channel. Different pipets of the same aperture size were used on different areas of the same film, or even on different films, which may lead to even larger variations in width and depth. The same is true for pipets of other aperture sizes. However, the volume etched must be proportional to the volume of trypsin delivered to the surface, and this does not depend on the

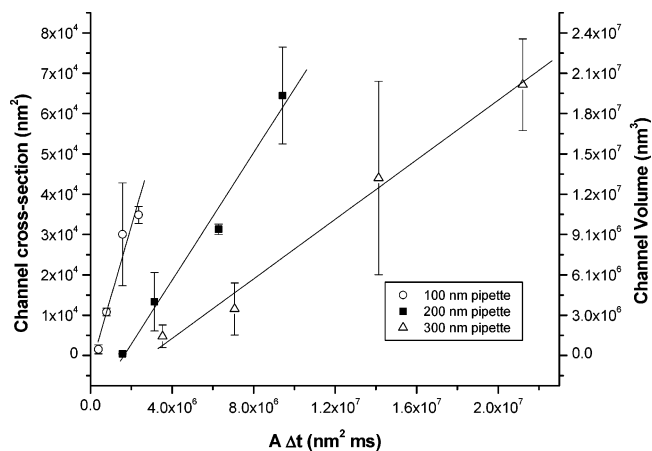


Figure 5. Dependence of channel cross-section on the volume of trypsin solution delivered. On the horizontal axis we plot $A\Delta t$ (area of the pipet aperture times dwelling time). On the left vertical axis we plot the channel cross-sectional area, calculated from the AFM images. The right vertical axis is the unit volume of the channel, calculated as the channel cross section area multiplied by the “pixel” size in the longitudinal direction along the channel. This is a constant and equals 300 nm for all experiments. The plots are expected to be linear (see text). Graphs are shown for three pipet diameters: 100 nm (open circles), 200 nm (closed squares), and 300 nm (open triangles). The linear fits (for the left vertical axis, i.e., channel cross-section) yield: $Y = (0.017 \pm 0.003)X - (3067 \pm 4799)$ for 100 nm pipets; $Y = (0.0080 \pm 0.0007)X - (13\,000 \pm 4451)$ for 200 nm pipets, and $Y = (0.0037 \pm 0.0002)X - (10\,547 \pm 3627)$ for 300 nm pipets.

position on the sample, which explains why the data look consistent when presented this way.

The data presented in Figure 5 split into three different linear slopes for the three different pipet apertures, where the steepest slope belongs to the smallest aperture (100 nm) and the shallowest slope belongs to the largest aperture (300 nm). The explanation for this fact is not straightforward, but we can suggest two possibilities. The slope of the graphs describing the channel volume (right vertical axis in Figure 5) is given, according to our model, by KV_L , where K is the ratio of volume etched to the volume of trypsin delivered and V_L is the linear velocity at which the solution flows out of the pipet, or KV_L/Ps , for the left vertical axis, where Ps is constant ($\sim 300 \text{ nm}$). The conclusion from the data in Figure 5 is that the product KV_L is different for pipets with different aperture diameters and it decreases with increasing aperture diameter. This can result from the change in either V_L or K (or both). V_L may be slower for pipets with a larger aperture diameter; since the rate of flow out of the pipet is governed by capillary forces and the strength of capillary forces decreases with increasing diameter of the pipet, this may be a plausible explanation. K , the ratio between the volume etched and the volume of solution delivered, is not necessarily a constant across different diameter pipets. The etching process stops when the water evaporates and renders trypsin inactive, as we have previously shown.² The evaporation rate of the water depends on the surface area of the drop, so that a drop with a large surface area will evaporate faster than a drop with a smaller surface area and the same volume. Therefore, if the same volume of trypsin is delivered with a

100 nm pipet or a 200 nm pipet (for example, a 100 nm pipet with $\Delta t = 200$ ms and a 200 nm pipet with $\Delta t = 50$ ms have equal products $A\Delta t$), and if the 200 nm pipet delivers this volume over a larger surface than the 100 nm pipet (due to the larger aperture), the water in the 200 nm case would evaporate faster, therefore ending the etching process earlier than in the 100 nm pipet case. This could explain why K for a 200 nm pipet would be lower than K for a 100 nm pipet, and so on. In principle, such an explanation is invalid for the case of a drop of liquid on a surface, when infiltration of the liquid does not occur. It is impossible to have drops with the same volume but different surface areas, because this would mean a different contact angle between the liquid and the surface, a property that is completely determined by the liquid and the surface (this also means that the sketch in Figure 1 would be wrong, in such conditions). However, in our case the BSA film is porous and is swelling, as we have already shown; therefore, penetration of water into the surface is certain. In such a case it is not impossible to have the diameter of the drop “pinned” at the value of the aperture diameter, since the liquid cannot “slide” on the surface in order to acquire the energetically favorable surface area. Therefore, it is not impossible that indeed same volumes of trypsin solution are covering larger areas when delivered with larger aperture pipets, leading to a faster evaporation and an earlier end of the etching process. Which of the effects is dominant, or whether the explanation is found in yet a different effect, is difficult to determine at this point. The conclusion, however, is clear from the experimental data: the etching efficiency (etched volume/delivered solution volume) is higher with smaller aperture pipets.

Having mapped this space, we can design the cross-section of channels (but not the width and depth separately), using one of the combinations pipet diameter/delay time.

As a side note, the concentration of trypsin is in principle also a parameter that can be varied in order to study the dependence of the channel geometry in response to it. However, from our experience, the practical range of concentration is very small. Considerably smaller concentrations slow the etching rate and, since this is a process that competes with swelling, one ends up with ridges² for a reduction of 50% in concentration (swelling “wins”). Increasing the concentration much above that used here leads to ridges too, presumably due to autolysis (self-cleaving) of trypsin which leads to deactivation. Therefore, we kept the concentration constant, at 2 mg/mL, throughout the experiments.

Etching is Additive. Further experiments show that the etching effect is “additive”, in the sense that an area etched once can be etched again with the same efficiency and governed by the same mechanism. As an example, we present an intersection of two perpendicular channels, in Figure 6. The “horizontal” channel (marked “1”) was created first, and the “vertical” channel (marked “2”) was created approximately 1 h later (long after drying of the trypsin solution that created the first channel). We present cross-sections along the lines indicated in the image in Figure 6b.

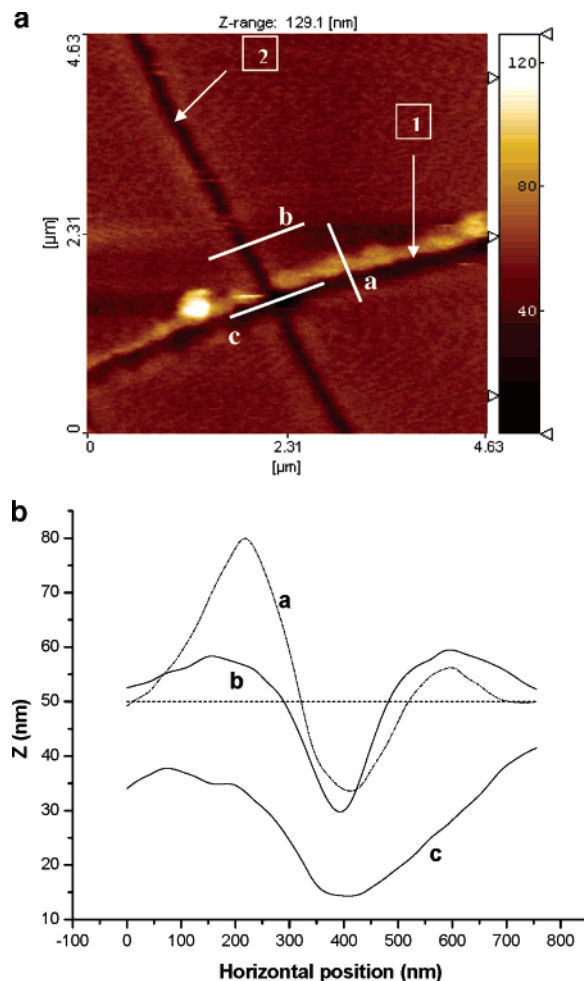


Figure 6. Intersection of two channels created with the same pipet at the same velocity. The horizontal channel (marked “1”) was created first and the vertical channel (marked “2”) was created later. Three cross-sections are presented in Figure 6b, along the lines indicated in Figure 6a. The dotted horizontal line in Figure 6b represents the original surface that had not swollen. It is observed that the dimensions of the channels are similar and that the depth of the depression at the intersection is the sum of depths of the channels.

The cross-section along line **a** shows the profile of the channel created first (1), the one along line **b** shows the profile along the channel created second (2), and the one along line **c** shows the profile of the “well” created at the intersection. The horizontal dotted line marks the position of the original BSA surface (which did not swell). The following facts are readily observed: both channels have very similar dimensions, since both were created with the same pipet and same writing parameters. The depth (measured in all cases from the original surface) shown by line **a** is ~ 17 nm, the depth shown by line **b** is ~ 20 nm, and the depth of the well (from the original BSA surface) is ~ 36 nm, which is the sum of depths of the channels. The depth of the well, measured relative to the floor of the horizontal channel (1), is ~ 20 nm, just like the depth of the vertical channel (2). The well is slightly wider in the horizontal direction than both channels (but not in the vertical direction) because the horizontal channel (1) existed already when the vertical

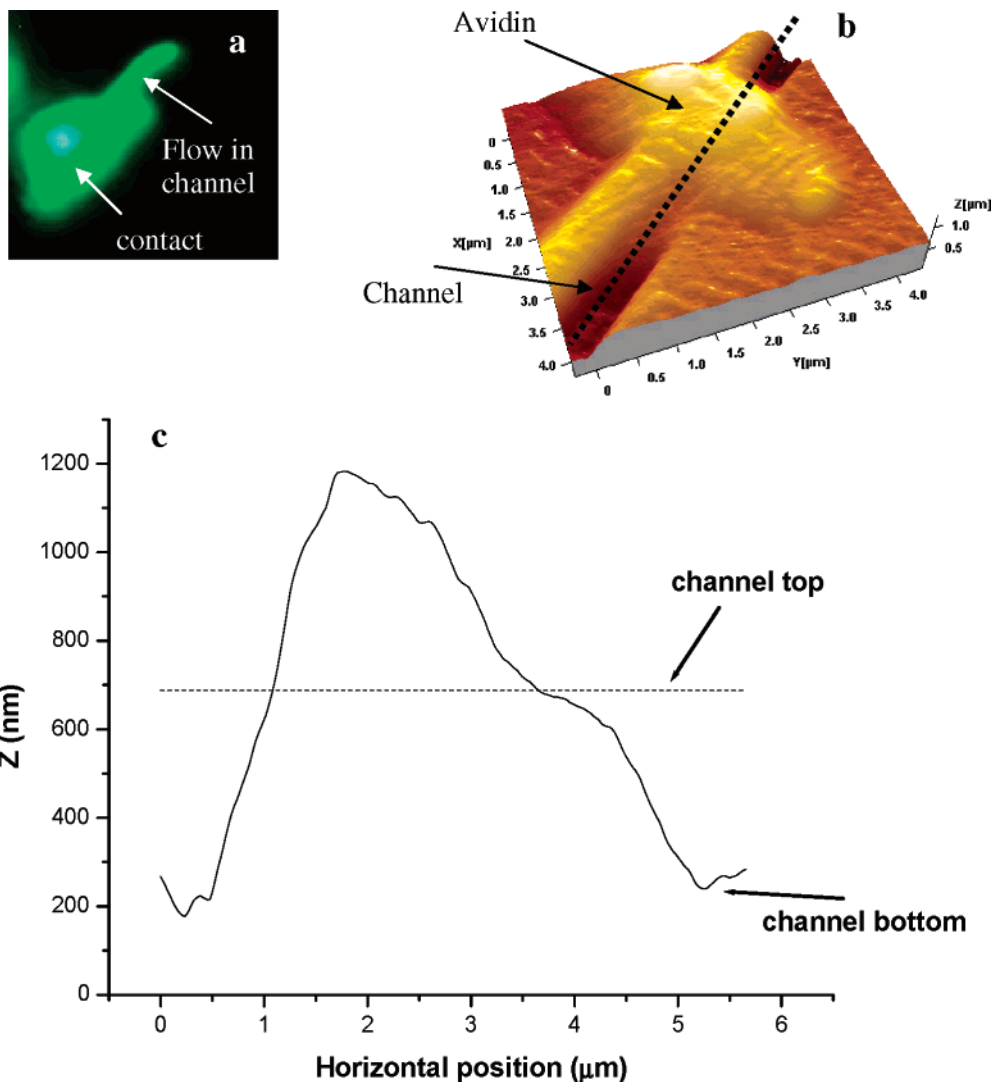


Figure 7. Fluorescently labeled avidin was flown into channels crated into a biotinylated BSA film. (a) Fluorescence microscope image showing the contact point and the fluorescence along the avidin filled channel. (b) AFM image showing cases where avidin flows only to a limited extent into the channel. (c) Profile along the dotted line in (b), showing the avidin filling the channel.

channel (2) was created, so some trypsin solution could flow into the horizontal channel and enlarge the depression.

The question arises, why is the trypsin that is already present on the substrate as a result of the first channel created not reactivated when it is re-hydrated upon writing the second channel? The fact that it is not is apparent from the perfectly additive result. The answer is that probably during drying it loses its conformation and function permanently, which also explains the stability of the features created over time (several months as far as we verified).

Flowing Protein Solution through the Channel. We further attempted to flow a protein solution through these channels. First the channels were created in a biotinylated BSA film, allowed to dry, and then another pipet was filled with fluorescently labeled avidin and was contacted with the channels. In few cases, upon contact with the channel, avidin filled it due to capillary forces. Such an example is shown in Figure 7a. However, in many other cases, although there was certain contact between the avidin-filled pipet and channels, there was no flow of avidin along the channels.

We investigated the areas of contact with AFM and revealed that avidin does flow to a very limited extent into the channel (Figure 7b,c); however, most of it builds up in a mound. We suspect the reason is that the BSA is swelling and absorbing the water, so that instead of flow along the channels, we get absorption into the BSA film.

Estimation of the Number of Molecules Involved in the Etching Process. Finally, we make a few estimations to get some understanding about the number of molecules participating in this process and the time scales involved.

Trypsin Activity. The activity of trypsin has been characterized by the manufacturer and reported as 270 TAME units/mg dry weight (at 25 °C). Activity of one TAME unit means that one μmol of *p*-toluene-sulfonyl-L-arginine methyl ester (TAME) is hydrolyzed in one minute. TAME has exactly one cleavage site (arginine) for trypsin, meaning that one unit of trypsin hydrolyzes 6×10^{17} substrate bonds/min (6×10^{23} molecules/mol $\times 10^{-6}$ mol/μmol), and since the activity is 270 units/mg, the rate of cleavage per unit weight of the trypsin used here is 1.6×10^{20} substrate bonds/min/

mg trypsin. Given trypsin's molecular weight of 23 000 g/mol, this amounts to 100 substrate bonds/s/trypsin molecule.

On the other hand, our measure of trypsin activity is the etched volume, and this is the result of a competition between swelling and "pure" etching, as we have shown previously. The value we have calculated above is the "pure" rate of etching, and, in order to account for the competition process (which causes a slower apparent activity), we note that² with the same trypsin concentration, the "pure" etching rate is four times faster than the swelling rate, and therefore the net etching rate is three times faster than the swelling rate. In light of these facts, we estimate the net etching rate of trypsin (pure etching minus swelling rate) as 75% of that calculated above, i.e., ~ 75 bonds/s/trypsin molecule, and this is the rate that we are indirectly measuring from the channel cross-section.

BSA Substrate. A BSA molecule has 86 lysine and arginine amino acids, which are specific cleavage sites for trypsin. Therefore, if all the bonds of BSA need to be hydrolyzed in order for it to collapse (obviously an overestimation), then BSA molecules collapse at a rate of 1.16 BSA molecule/trypsin molecule/s (one molecule of trypsin hydrolyzes all the lysine and arginine bonds of one BSA molecule in slightly less than one second). Moreover, assuming a BSA molecule is a sphere with a radius of 3 nm, thus it frees a volume of $\sim 10^{-7} \mu\text{m}^3$ when it collapses, one gets an etching rate of $\sim 10^{-7} \mu\text{m}^3/\text{s}/\text{trypsin molecule}$. The BSA molecules, however, are not closely packed in the dried film, therefore a BSA molecule that collapses should free a volume considerably larger than its own. Both the overestimation of the number of bonds that need to be cleaved to cause a collapse and the underestimation of the volume freed by a collapsed BSA molecule lead to an underestimation of the etching rate of trypsin. In an attempt to correct for this, we note the following: the packing density of spheres in cubic packing (where the spheres are stacked directly on top of each other) is $P \cong 0.524$. This means that 47.6% (almost half) of the space occupied by spheres arranged this way is empty. Hexagonal packing is more efficient, giving only $\sim 26\%$ empty space. However, since our dried film does not have a crystal structure, it is not likely to have such high packing densities. Random packing of spheres gives packing ratios in the range 0.06 to 0.65.^{11,12} For the purpose of the present estimation we will assume a 50% packing density, so that a BSA molecule will be assumed to free $2 \times 10^{-7} \mu\text{m}^3$ when it collapses. Furthermore, we will also assume only ~ 30 bonds (out of 86 possible) need to be cleaved in order for a collapse to occur.

Interpretation of the Measurements. The slopes of the graphs in Figure 5 contain an important piece of information that can be further analyzed. Focusing for example on the graph describing the 100 nm aperture pipet, we see a slope of 0.017 ms^{-1} , which equals the product KV_L/P_s or $KV_L \approx 5 \mu\text{m/s}$. From this observation alone we can get an idea about the value of K , the ratio between the volume of solution delivered and the etched volume (the "efficiency", as we called it previously). K must be greater than 1: the writing

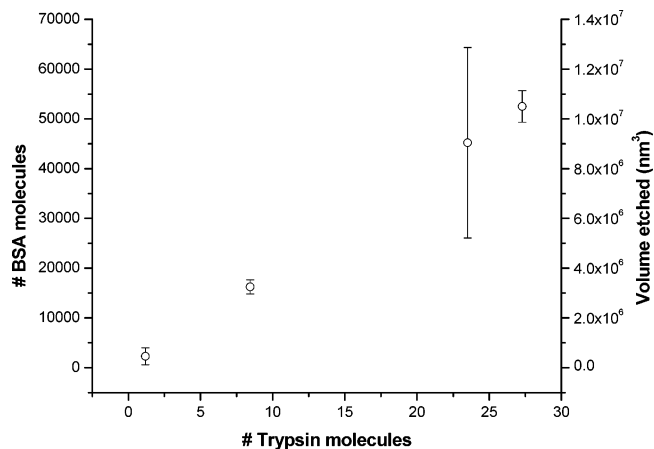


Figure 8. Translation of the graph in Figure 5 for the 100 nm pipet into number of trypsin molecules deposited (horizontal axis) and number of BSA molecules etched (vertical axis), according to the estimation presented in the text.

of one line $77 \mu\text{m}$ long, even at the fastest velocity ($\Delta t = 50 \text{ ms}$), takes 12.8 s ($256 \text{ pixels} \times 50 \times 10^{-3} \text{ s/pixel}$), i.e., if K would have been of the order of 1, the level of trypsin solution in the pipet would have decreased by $64 \mu\text{m}$ (at $V_L \approx 5 \mu\text{m/s}$) during the writing of a single channel. This is impossible, since the length of the pipet filled with solution (observed with a light microscope) is $\sim 100 \mu\text{m}$, and we are able to write tens of such channels without refilling. Thus, V_L should be smaller than $5 \mu\text{m/s}$, by at least 1 order of magnitude (which would allow writing of tens of channels). This would force $K \sim 10$. To remind, $K \equiv (\text{volume etched})/(\text{volume deposited})$, meaning that we are etching a volume ~ 10 times larger than the volume of trypsin solution deposited.

In fact, once this observation is made, it sets an absolute number of trypsin molecules that are participating in the etching process. First, let us note that the concentration of $\sim 1 \text{ mg trypsin/mL}$ solution we have used is equivalent to $\sim 0.26 \times 10^{-4} \text{ trypsin molecules/nm}^3$. Then, having set $K = 10$, we calculate the volume of solution deposited as the etched volume divided by K and multiply by the concentration above to get the number of trypsin molecules deposited. The graph in Figure 8 presents these data for the 100 nm aperture pipet on the ordinate (x) axis. Note that the smallest volume ($\sim 0.2 \times 10^6 \text{ nm}^3$) has been etched by only ~ 5 trypsin molecules, while the largest one, by ~ 30 molecules.

From the earlier discussion we assume that each BSA molecule frees $2 \times 10^{-7} \mu\text{m}^3$, therefore we can translate the etched volume to number of BSA molecules. These data are presented in Figure 8, left y axis. The slope of a linear regression fit through the points is 1920 BSA molecules/trypsin molecule. In other words, each trypsin molecule caused the collapse of approximately 1900 BSA molecules during as long as it took the water to evaporate. If we take the trypsin activity above, then 1 trypsin molecule hydrolyzes 75 bonds per second, so the disappearance of 1920 BSA molecules (assuming just ~ 30 bonds need to be hydrolyzed) should take some 12 min. Therefore, the scenario emerging from these estimations is as follows. On each of 256 steps,

300 nm apart, $0.2\text{--}1.1 \times 10^6 \text{ nm}^3$ (or $0.2\text{--}1.1 \times 10^{-3}$ femtoliter) of solution is flown through the 100 nm diameter aperture during 50–300 ms (at a linear velocity of $0.5 \mu\text{m/s}$), evaporates within ~ 12 min, during which each one of 5–30 trypsin molecules manage to cleave 30 bonds on each of 1900 BSA molecules, which collapse as a result, and free a volume of $2 \times 10^7 \text{ nm}^3$ (or 2×10^{-2} femtoliter) each.

To conclude, we have shown the following. (i) Control of the writing velocity and aperture diameter of the pipet only are sufficient to control the dimensions of the channels. This makes the technique extremely simple and avoids the need for humidity control (as in the DPN technique³) or immobilization of the enzyme to the AFM probe and working in (aqueous) solution, in the other reported case.¹ (ii) It is difficult to control width and depth of channels separately in this system, probably due to anisotropy of the film. In some cases, where the film is isotropic and homogeneous, it has been shown that such a possibility still exists. The careful creation of a homogeneous substrate should make it possible always. (iii) The control of channel cross-section, on the other hand, has been shown to be very precise. (iv) It has been shown that in certain conditions only a few (~ 5) trypsin molecules are delivered in each position, making the method comparable with AFM tip tethered enzymes,¹ in this respect. (v) Etching has been shown to be additive, in the sense that an area once etched can be etched again, governed by the same mechanism. (vi) It is possible to flow solutions of protein through channels manufactured this way, although swelling of the substrate makes the process unpredictable.

The characterization of the trypsin-BSA model system with NFP led to a good understanding of the process. In the next

step, efforts will be invested into careful design of appropriate substrates that are both homogeneous and not subject to swelling. This will allow the development of nanofluidic systems.

Acknowledgment. This work has been partially supported by grant #346/00 from the Israel Science Foundation and grant #01-01-01328 from the Israel Ministry of Science, Culture and Sports.

References

- (1) Takeda, S.; Nakamura, C.; Miyamoto, C.; Nakamura, N.; Kageshima, M.; Tokumoto, H.; Miyake, J. *Nano Lett.* **2003**, *3*, 1471.
- (2) Ionescu, R. E.; Marks, R. S.; Gheber, L. A. *Nano Lett.* **2003**, *3*, 1639.
- (3) Hyun, J.; Kim, J.; Craig, S. L.; Chilkoti, A. *J. Am. Chem. Soc.* **2004**, *126*, 4770.
- (4) Piner, R. D.; Zhu, J.; Xu, F.; Hong, S. H.; Mirkin, C. A. *Science* **1999**, *283*, 661.
- (5) Lewis, A.; Kheifetz, Y.; Shambrodt, E.; Radko, A.; Khatchatryan, E.; Sukenik, C. *Appl. Phys. Lett.* **1999**, *75*, 2689.
- (6) Bruckbauer, A.; Ying, L. M.; Rothery, A. M.; Zhou, D. J.; Shevchuk, A. I.; Abell, C.; Korchev, Y. E.; Klenerman, D. *J. Am. Chem. Soc.* **2002**, *124*, 8810.
- (7) Demers, L. M.; Ginger, D. S.; Park, S. J.; Li, Z.; Chung, S. W.; Mirkin, C. A. *Science* **2002**, *296*, 1836.
- (8) Taha, H.; Marks, R. S.; Gheber, L. A.; Rousso, I.; Newman, J.; Sukenik, C.; Lewis, A. *Appl. Phys. Lett.* **2003**, *83*, 1041.
- (9) Liu, G. Y.; Amro, N. A. *Proc. Natl. Acad. Sci. U.S.A.* **2002**, *99*, 5165.
- (10) Lee, K. B.; Park, S. J.; Mirkin, C. A.; Smith, J. C.; Mrksich, M. *Science* **2002**, *295*, 1702.
- (11) Jaeger, H. M.; Nagel, S. R. *Science* **1992**, *255*, 1523.
- (12) Torquato, S.; Truskett, T. M.; Debenedetti, P. G. *Phys. Rev. Lett.* **2000**, *84*, 2064.

NL0500510